Miniaturized Wire Trap for Neutral Atoms

J. Fortagh, A. Grossmann, and C. Zimmermann
Physikalisches Institut, Eberhard-Karls-Universität, Auf der Morgenstelle 14, 72076 Tübingen, Germany

T. W. Hänsch
Sektion Physik, Ludwig Maximilians Universität, Schellingstraße 4, 80799 München, Germany
and Max-Planck Institute of Quantum Optics (MPQ), 85740 Garching, Germany
(Received 3 August 1998)

We demonstrate the loading of a miniaturized magnetic guide for neutral atoms made of small-size current conductors. Cold rubidium atoms are initially stored in a shallow spherical quadrupole field and subsequently transferred into the magnetic guide by gradually transforming the trapping potential. Density, temperature, and atom number have been monitored *in situ* by absorption imaging with a charge-coupled device camera. A fraction of 14% of the initially trapped atoms has been transferred into the linear microtrap at a temperature of 39 μK. [S0031-9007(98)07972-1]

PACS numbers: 39.90.+d, 03.75.Fi, 52.55.Lf

In recent years, the magnetic trapping of neutral atoms has been developed into a key technique for a rapidly growing number of spectacular experiments with ultracold atoms. Because of their outstanding thermal isolation properties, magnetic traps are particularly suitable for cooling atomic clouds down to record temperatures [1]. On the other hand, the magnetic trapping force can be made sufficiently strong to confine single atoms or atomic ensembles to very small volumes [2]. If strong confinement and low temperature are combined, nonclassical behavior of the single particle motion is expected for a thermal energy of the trapped atom smaller than the energy separation between adjacent vibrational levels. Under these conditions, the external motion of the atoms must be treated quantum mechanically, and one obtains a promising new testing ground for the investigation of fundamental quantum effects. In particular, magnetic guides may be realized in which the atomic matter waves propagate in the transverse ground state analogous to electronic quantum wires or optical single mode fibers. Intriguing applications are conceivable in atom interferometry, in quantum computation [3], for the construction of a continuous source of coherent matter waves [4], and for the study of one-dimensional quantum gases [5].

Tightly confining magnetic potentials can be realized, in principle, by miniaturizing the elements which generate the magnetic field. Weinstein and Libbrecht have proposed microscopic traps based on combinations of current conductors which can be made extremely small by standard microfabrication techniques [6]. However, these traps suffer from a minute trapping volume which is difficult to load with a substantial number of atoms. So far, such microtraps have not been filled with atoms although the magnetic "hardware" has already been demonstrated [7]. In this Letter, we describe the first loading of a wire trap of the Libbrecht type by means of adiabatic transport and compression. The key feature of the experiment is a novel scheme for gradually transforming a spherical quadrupole trap with a large trapping volume into the geometry of a microtrap.

In our experiment, the microtrap is formed by a linear quadrupole potential which can be realized by combining the circular field of a wire conductor with a homogeneous bias field oriented perpendicular to the wire axis. The two magnetic fields exactly compensate along a line which forms the center of a linear quadrupole field parallel to the wire. For decreasing current in the wire, the center line of the trap approaches the wire surface and the gradient of the potential increases. The gradient may reach very large values limited only by the finite size of the wire. In our setup (Fig. 1), we use a vertically oriented thin copper wire (45 μm radius) that is cemented onto the surface of a parallel thick wire (750 μm radius). The thin wire is electrically insulated and can carry up to $I_W = 3$ A with the dissipated heat drained by the thick

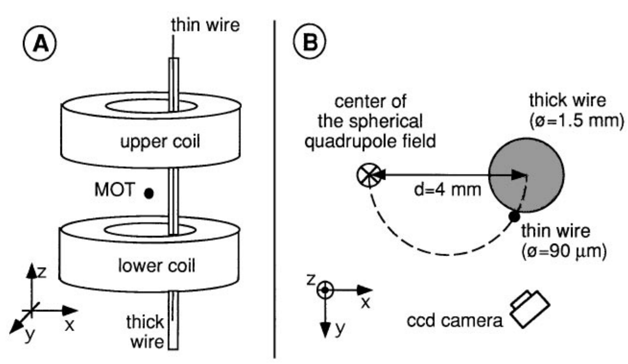

FIG. 1. (a) Trap setup consists of two coils and a pair of wire conductors oriented parallel to the symmetry axis of the coils. (b) Position of the wires in the x-y plane. The center of the thick wire and the center of the spherical quadrupole field define the base of a half circle (dashed line). At the position of the thin wire, the half circle intersects the surface of the thick wire.

 0031-9007/98/81(24)/5310(4)$15.00

wire. The setup is completed by a pair of coils arranged in the anti-Helmholtz configuration. It generates a spherical quadrupole field which serves for the operation of a magnetro-optical trap and for initially trapping the atoms before they are loaded into the wire trap. The symmetry axis of the spherical quadrupole field is oriented parallel to the wires but it is displaced relative to the center of the thick wire by $d = 4$ mm. At the position of the thin wire, the anti-Helmholtz coils provide an approximately homogeneous bias field. The combination of the bias field and the field of the thin wire forms the microwire trap.

To transfer the atoms into the wire trap, the current in the thick wire I_{th} is slowly increased. As a consequence, the centers of both the spherical quadrupole and the wire trap move within the horizontal plane and approach each other on a circular trajectory (Fig. 2). At a critical current I_c, the centers merge and form a Ioffe-type trap [8] with vanishing offset field. If the current in the thick wire exceeds I_c, an offset field is added to the trap minimum and the classical Ioffe trap geometry is completed. This surprisingly simple realization of a Ioffe trap forms the basis of our loading scheme: The empty wire trap can be loaded from the filled shallow quadrupole by simply merging both trap minima at $I_{\mathrm{th}} > I_c$. After the coalition, the current in the thick wire is slowly reduced back to zero and a part of the atoms is transferred into the wire trap while the remainder is again stored in the central shallow quadrupole. The procedure is quasiadiabatic in the sense that the phase space density is reduced only by a constant factor due to the splitting of the atomic cloud into two parts. This factor can be close to unity, if one of the two volumes is small. The verification of the loading scheme is the purpose of the experiment presented in this Letter.

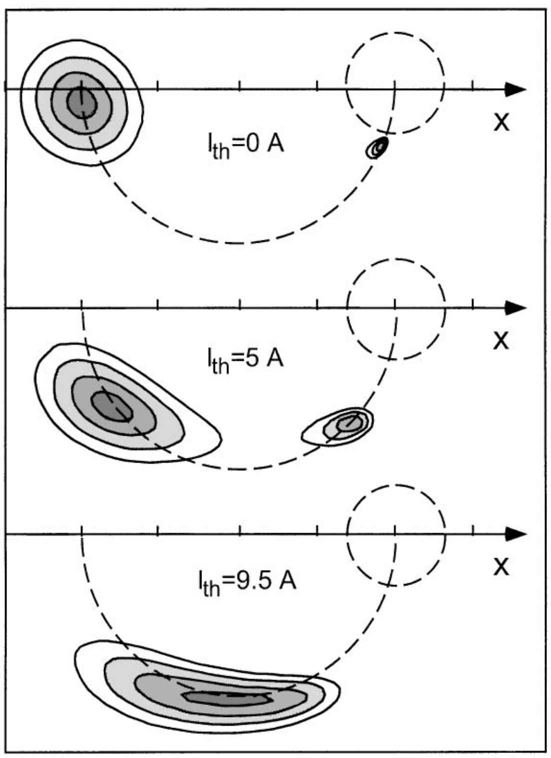

FIG. 2. Loading the wire trap: Numerically calculated contour line plot of the two potential minima in the x-y plane at three different currents in the thick wire. The current in the thin wire is set to a constant value of 1.4 A. The contour lines are plotted up to a magnetic field strength of 2 G at an increment of 0.5 G. The dashed circle indicates the cross section of the thick wire. The thin wire is not shown. The atoms are initially stored at $I_{\mathrm{th}} = 0$ A in the shallow tap minimum on the left side of the plot. By increasing the current in the thick wire to 9.5 A, the two minima move on a circular trajectory (dashed half circle) and finally merge to a Ioffe-type trap. After I_{th} has been slowly reduced back to 0 A, about 14% of the atoms have been transferred into the steep potential minimum close to the thin wire.

Before the experiment is described in detail, we shortly summarize the trap parameters of the Ioffe trap which can be derived analytically, if the field of the coils is approximated by an ideal spherical quadrupole and the two wires are represented by a single wire that is assumed to be infinitesimally thin. The critical current at which the two trap minima coalesce and the Ioffe trap is formed is then given by $I_c = \pi b_z d^2/2\mu_0$. Here, b_z denotes the gradient dB/dz of the magnetic field modulus B along the positive z axis. At the critical current ($I_{\mathrm{th}} = I_c$), the potential minimum of the Ioffe trap is located halfway between the center of the coils and the thick wire. For the curvature of the magnetic field modulus along the slow axis (x axis) of the Ioffe trap, one obtains $d^2B/dx^2 = 3b_z/d$, while the gradient along the y axis amounts to $dB_y/dy = -dB_z/dz = b_z$. At currents I_{th} between 0 and I_c, the x coordinates of the two trap minima are given by $x = (d/2)(1 \pm p^{1/2})$ with $p = 1 - (I_{\mathrm{th}}/I_c)^2$. The depth of the two trapping potentials is limited by the potential barrier that separates the two traps. As the current I_{th} is varied, the saddle point of the barrier moves on a straight line between the wire and the center of the intermediate Ioffe trap. The magnetic field modulus at the saddle point may be written as $B_s = (1/2)b_z(d - \sqrt{2}\,q)$. The length parameter q is given by $q = \sqrt{\mu_0 I/\pi b_z}$ and describes the distance between the wire and the position of the saddle point in the horizontal plane. In our setup, the coils provide an axial gradient b_z of 51 G/cm which leads to an estimation for the critical current and the curvature of the Ioffe trap potential of $I_c = 8$ A and $d^2B/dx^2 = 383$ G/cm^2, respectively. For rubidium in a harmonic potential, the curvature of 383 G/cm^2 corresponds to an oscillation frequency of 34 Hz.

In our experiment, rubidium atoms (^{87}Rb) are collected and cooled in a magneto-optical trap (MOT) to a temperature of 30 μK ($b_z = 18$ G/cm, 2 mW laser power in each of the six laser beams with 6 mm beam diameter each). The MOT is operated in an ultrahigh vacuum chamber at a residual gas pressure of smaller than 10^{-9} mbar. As a source for the thermal rubidium atoms, we use a commercially available continuously driven alkali dispenser which has been described elsewhere [9]. The atoms are loaded from the MOT into the trapping potential of the central quadrupole by blocking the laser light and suddenly increasing the gradient to $b_z = 51$ G/cm. During the whole experiment, the current in the thin wire is set to a constant value of 1.4 A. The transfer into the wire trap occurs within 640 ms during which the current in the thick wire is slowly raised from 0 to 9.1 A and then slowly turned off. To avoid nonadiabatic heating, the current is varied at a time dependent rate such that the acceleration and the deceleration of the trap centers occur at a constant value of $0.06\ \mathrm{m/s^2}$. This is a conservative value and has not been optimized. The spatial distribution of the trapped atoms is monitored by illuminating the atomic cloud with a collimated laser beam and imaging the resonant absorption with a charge-coupled device (CCD) camera. Figure 3(a) shows four typical images taken at various times during the transport. The observation axis of the CCD camera is tilted relative to the y axis by 49°. From this observation angle, the atomic cloud appears to move only very little during the first half of the transfer. After 320 ms, the maximum current of 9.1 A is reached and the two trap potentials have merged and form a Ioffe trap with a nonzero offset field. For later times, a part of the atomic cloud separates into the wire trap where it is compressed along the horizontal coordinates. The fraction which is not transferred into the wire trap is again stored in the central quadrupole potential.

For quantitative analysis, we cut the absorption images horizontally and vertically with respect to the clouds peak density. By fitting the theoretically predicted curves to the experimental data, we derive the number of trapped atoms, the density, and the temperature of the atomic clouds before and after the transfer. The theoretical absorption profiles have been obtained by integrating the resonant absorption of a thermalized atomic cloud along the observation axis. Figure 4 gives an example for the absorption data after the transfer has been completed. Both the transferred and the restored part of the cloud are clearly separated, and the horizontal extension of the cloud in the wire trap is reduced by about a factor of 4 compared to the restored part of the cloud. Along the vertical direction (z axis) the absorption profile is influenced by gravity (inset of Fig. 4). In a linear potential, the trap minimum remains unshifted while the density distribution is asymmetrically distorted towards the gravitational force. This is in contrast to the parabolic potential of the intermediate Ioffe trap where the cloud shape remains symmetric but the position of the peak density experiences a shift due to gravity. We clearly observe this effect [Fig. 3(b)] which verifies the Ioffe-type geometry for the intermediate trap. The strength of the asymmetry reflects the ratio between the trapping potential $U(r)$ and the gravitational potential and can be used to calibrate $U(r)$ relative to the known magnetic field modulus $B(r)$. The data are consistent with $U(r) = 0.5\mu_B B(r)$, where μ_B is the Bohr magnetron. Since we could not observe any population in the states with $F = 1$, we conclude that the atoms are predominantly trapped in the state with $F = 2$, $m_F = 1$.

By analyzing the absorption data, we find that 6.3×10^6 atoms have been trapped magnetically at a peak density of $7.0 \times 10^9\ \mathrm{cm^{-3}}$ and a temperature of 32 μK before the transfer takes place. After the transfer, we observe 4.1×10^6 atoms in the spherical quadrupole at a peak density of $5.0 \times 10^9\ \mathrm{cm^{-3}}$ and a temperature of 32 μK. The fraction which has been transferred into the wire trap amounts to 6.9×10^5 atoms of a temperature of 39 μK and a peak density of $6.0 \times 10^9\ \mathrm{cm^{-3}}$. The statistical errors of the fitted parameters range between 5%–12%. The difference between the total number of

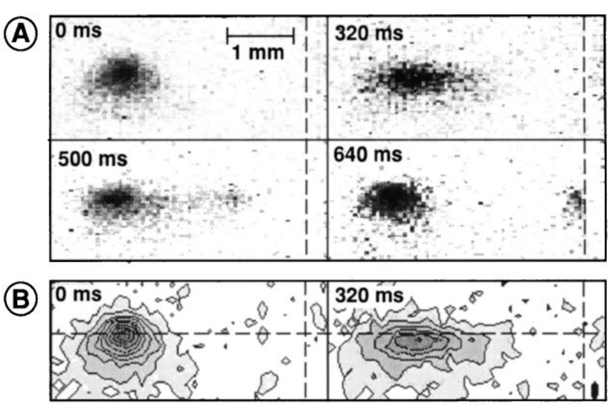

FIG. 3. (a) Absorption images at various times during the transfer into the wire trap. The vertical dashed line indicates the edge of the thick wire as seen from the camera perspective. (b) Contour plot of the same data. In a trap with linear potential, gravity causes an asymmetric cloud profile while in a parabolic potential the cloud remains symmetric but its center is shifted. The dashed horizontal line indicates the position of the cloud center in the linear potential trap.

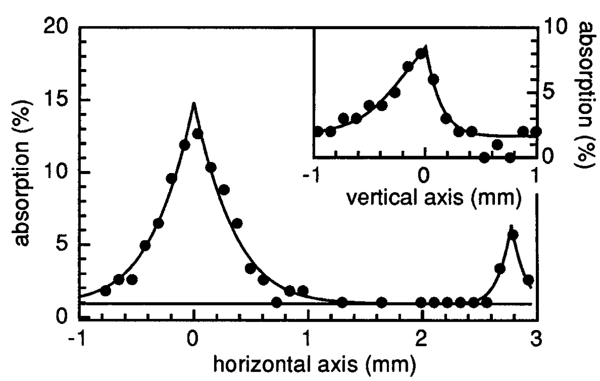

FIG. 4. Cuts through the absorption images. Before the cut is taken, the image has been averaged by binning four neighboring pixels. In the horizontal direction, the cloud in the wire trap is compressed by a factor of 4 relative to the distribution inside the central quadrupole. The inset shows the vertical distribution of the atoms in the wire trap which is asymmetrically distorted due to gravity.

atoms before and after the transfer is consistent with losses due to collisions with the background gas which limit the trap lifetime to 2.3 s. The efficiency of the transfer into the wire trap is thus 14%. The phase space density in the wire trap has been reduced by a factor of 0.64 relative to the initially trapped cloud. After correcting for collisional losses, we find that the transfer reduces the phase space density only by a factor of 0.82. It is instructive to compare this value to the case of two box potentials that are merged and separated in a similar way. There, the phase space density in the merged trap is reduced by $1 - N_2/N_1$ relative to the phase space density in the initially filled trap. Here, N_2/N_1 is the fraction of atoms that has been transferred into the smaller, initially empty trap. A transfer efficiency of 14% causes a reduction of phase space density of 0.86 which is close to our observed value of 0.82. In our experiment, the two clouds are separated by the potential barrier that gradually grows while the current in the thick wire is reduced to zero. During this part of the transfer, the more energetic atoms pass the barrier such that only the atoms with low energy remain inside the wire trap. As a consequence, the temperature inside the wire trap increases only slightly despite the considerable compression of the cloud size. At the end of the transfer, the height of the barrier is 1.3 times larger than the average energy of the cloud inside the wire trap such that most of these atoms are now confined near the wire.

After the transfer, the cloud can be further compressed by slowly inverting the current in the thick wire. Because of its larger diameter, the field of the thick wire is approximately constant on the scale of the trap size. It contributes to the bias field of the coils and eventually dominates it such that the coils can be turned off. With the current setup, we cannot observe this additional compression since, for negative currents in the thick wire, the atomic cloud is hidden in the shadow of the thick wire and becomes invisible for the CCD camera. We conclude this Letter by briefly discussing the expected properties of a compressed trap at current values which can be realized with the present setup. For $I_{\mathrm{th}} = -19$ A and $I_w = 2.5$ A, the trap center is displaced 25 μm from the surface of the thin wire and the trap depth is limited by the magnetic field strength at the surface to 35 G. The gradient at the trap center amounts to 3700 G/cm and the temperature of the atomic cloud is expected to increase to 200 μK during compression. The compressed wire trap can be adiabatically transformed into a Ioffe-type geometry by slowly inverting the current in the upper coil. When the current goes through zero, the magnetic confinement of the atoms in the upward direction disappears. However, for rubidium trapped in a hyperfine ground state with $|m_F| = 1$, gravity is equivalent to a potential generated by a magnetic field gradient of 15 G/cm. This is sufficient to prevent a substantial expansion of the cloud in the vertical direction.

In summary, we have demonstrated a novel scheme for loading miniaturized magnetic traps. Starting with cold rubidium atoms from a magneto-optical trap, 7×10^5 atoms have been transferred into the quadrupole potential of a microwire trap at a temperature of 39 μK. In combination with very recently reported microelectromagnets [7], our loading scheme may help to realize intriguing scenarios of atomic ensembles guided and manipulated in microscopic structures.

We gratefully acknowledge helpful discussions with Vladan Vuletic and Axel Görlitz. This work is supported in part by the Deutsche Forschungsgemeinschaft (Zi 419/2).

[1] M. H. Anderson *et al.*, Science **269**, 189 (1995); K. B. Davis *et al.*, Phys. Rev. Lett. **75**, 3969 (1995); C. C. Bradley *et al.*, Phys. Rev. Lett. **75**, 1687 (1995); see also, Georgia Southern University BEC home page, http://amo.phy.gasou.edu.bec.html

[2] V. Vuletic, T. Fischer, M. Praeger, T. Hänsch, and C. Zimmermann, Phys. Rev. Lett. **80**, 1634 (1998).

[3] I. Cirac and P. Zoller, Phys. Rev. Lett. **74**, 4091 (1995); D. M. Meekhof, C. Monroe, B. E. King, W. M. Itano, and D. J. Wineland, Phys. Rev. Lett. **76**, 1796 (1996).

[4] U. Janicke and M. Wilkens, Europhys. Lett. **35**, 561 (1996); J. I. Cirac, M. Levenstein, and P. Zoller, Europhys. Lett. **35**, 647 (1996).

[5] J. Voigt, Rep. Prog. Phys. **57**, 977 (1994); N. J. van Druten and W. Ketterle, Phys. Rev. Lett. **79**, 549 (1997); M. Olshanii, Phys. Rev. Lett. **81**, 938 (1998).

[6] J. D. Weinstein and K. G. Libbrecht, Phys. Rev. A **52**, 4004 (1995).

[7] M. Drndic *et al.*, Appl. Phys. Lett. **72**, 2906 (1998); K. S. Johnson *et al.*, Phys. Rev. Lett. **81**, 1137 (1998); J. Reichel, W. Hänsel, C. Sartena, and T. W. Hänsch, in *Technical Digest, Proceedings of the Conference on EQEC 1998, Glasgow* (IEEE Service Center, Piscataway, NJ, 1998).

[8] T. Bergeman, G. Erez, and H. J. Metcalf, Phys. Rev. A **35**, 1535 (1987).

[9] J. Fortagh, A. Grossmann, T. W. Hänsch, and C. Zimmermann, J. Appl. Phys. (to be published).